Supporting Online Material (SOM)

for

"A Genetic Screen in *Drosophila* for Metastatic Behavior"

Raymond A. Pagliarini and Tian Xu

Materials and Methods

Strains

Flies were cultured at 25 C on standard medium. The genotypes for the animals described in the text are listed below, along with the number of animals (n) dissected and analyzed for ventral nerve cord invasion in Figure 2.

For the F2 mosaic screens, *w*; *UAS-Ras^{V12}*; P[FRT]82B males were mutagenized and crossed with *w*; *UAS-Ras^{V12}*; *Sb*/*TM6B* females to obtain individual mutant lines balanced on the third chromosome. Alternatively, pre-existing mutations on 3R were recombined onto an FRT chromosome, and *UAS-Ras^{V12}* was placed on the second chromosome. These lines were crossed with *y,w,eyFLP1*; *Act5C>y^{+}>Gal4*, *UAS-GFP*/*UAS-Ras*^{V12}; P[FRT]82B *Tub-Gal80* females and analyzed with a Leica MZ FLIII fluorescence stereomicroscope.

UAS-scrib is an unpublished stock kindly given to us by David Bilder.

(Fig 1A) *y,w,eyFLP1*/*w* or Y; *Act5C>y^{+}>Gal4*, *UAS-GFP*/+; P[FRT]82B *Tub-Gal80*/ P[FRT]82B *lats^{X1}* (n>1000)

(Fig 2A) *y,w,eyFLP1*/*w* or Y; *Act5C>y^{+}>Gal4*, *UAS-GFP*/+; P[FRT]82B *Tub-Gal80*/ P[FRT]82B (n>1000)

(Fig 2B, 4C) *y,w,eyFLP1*/*w* or Y; *Act5C>y^{+}>Gal4, UAS-GFP*/UAS-Ras^{V12}; P[FRT]82B *Tub-Gal80*/ P[FRT]82B (n>1000)

(Fig 2C, 4A) *y,w,eyFLP1*/*w* or Y; *Act5C>y^{+}>Gal4, UAS-GFP*/+; P[FRT]82B *Tub-Gal80*/ P[FRT]82B, *scrib^{1}* (n=100)

(Fig 2D) *y,w*/*w* or Y; *ey-FLP5*, *Act5C>y^{+}>Gal4*, *UAS-GFP*; *scrib^{1}*/*Df (3) Tl-X* (n=10)

(Fig 2E, 2H, 3, 4B, 4D) *y,w,eyFLP1*/*w* or Y; *Act5C>y^{+}>Gal4, UAS-GFP*/ *UAS-Ras^{V12}*; P[FRT]82B *Tub-Gal80*/ P[FRT]82B, *scrib^{1} ^{orj7B3}* (n>200)

(Fig 2F) *y,w,eyFLP1*/*w, UAS-scrib*; *Act5C>y^{+}>Gal4, UAS-GFP*/ *UAS-Ras^{V12}*; P[FRT]82B *Tub-Gal80*/ P[FRT]82B, *scrib^{1}* (n=25)

(Fig 2G, 2I) *y,w,eyFLP1*/*w* or Y; *Act5C>y^{+}>Gal4*, *UAS-GFP*/*UAS-Ras^{V12}*; P[FRT]82B *Tub-Gal80*/ P[FRT]82B *lats^{XTN33A} or ^{X1}* (n=50)

(Fig 2J) *w,eyFLP1.2*/*w* or Y; *Act5C>y^{+}>Gal4, UAS-GFP*/ *UAS-Ras^{V12}*; P[FRT]82B *Tub-Gal80*/ P[FRT]82B, *scrib^{1}* (n=10)

(Fig 2K) *y,w,eyFLP1*/*w* or Y; *Act5C>y^{+}>Gal4*, *UAS-GFP*/*UAS-Ras^{V12}*, *UAS-DECH^{12}*; P[FRT]82B *Tub-Gal80*/ P[FRT]82B *scrib^{1}* (n=58)

(Fig 2L) *y,w,eyFLP1*/*w* or Y; *Act5C>y^{+}>Gal4*, *UAS-GFP*/UAS-*Ras^{V12}*, *UAS-CADH^{intra5}*; P[FRT]82B *Tub-Gal80*/ P[FRT]82B *scrib^{1}* (n=15)

(Fig 2M) *y,w,eyFLP1/w* or Y; P[FRT]43D *Tub-Gal80*/P[FRT]43D $shg^{2\ or\ k03401}$; *Act5C>y⁺>Gal4*, *UAS-GFP*/*UAS-Ras*^{V12} (n=21)

(Fig 2N) *y,w,eyFLP1/w* or Y; lgl^{4} P[FRT]40A *UAS-Ras*^{V12}/ *Tub-Gal80* P[FRT]40A (n=25)

(Fig 2O) dlg^{m52} P[FRT]19A / *Tub-Gal80* P[FRT]19A ; *eyFLP5*, *Act5C>y⁺>Gal4*, *UAS-GFP*/*UAS-Ras*^{V12} (n=28)

(Fig 2P) baz^{4} P[FRT]19A/ *Tub-Gal80* P[FRT]19A ; *eyFLP5*, *Act5C>y⁺>Gal4*, *UAS-GFP*/*UAS-Ras*^{V12} (n=14)

(Fig 2Q) sdt^{N5} P[FRT]19A/ *Tub-Gal80* P[FRT]19A ; *eyFLP5*, *Act5C>y⁺>Gal4*, *UAS-GFP*/*UAS-Ras*^{V12} (n=10)

(Fig 2R) $cdc42^{1}$ P[FRT]19A/ *Tub-Gal80* P[FRT]19A ; *eyFLP5*, *Act5C>y⁺>Gal4*, *UAS-GFP*/*UAS-Ras*^{V12} (n=10)

(Fig 2S) *y,w,eyFLP1/w* or Y; *Act5C>y⁺>Gal4*, *UAS-GFP*/ *UAS-p21*, *UAS-Ras*^{V12}; P[FRT]82B *Tub-Gal80*/ P[FRT]82B, $scrib^{1}$ (n=20)

(Fig 2T) *y,w,eyFLP1/w* or Y; *Act5C>y⁺>Gal4*, *UAS-GFP*/*UAS-E2F*, *UAS-Dp*; P[FRT]82B *Tub-Gal80*/ P[FRT]82B $scrib^{1}$ (n=8)

(Fig 2U) *y,w,eyFLP1/w* or Y; *Act5C>y⁺>Gal4*, *UAS-GFP*/*UAS-p35*; P[FRT]82B *Tub-Gal80*/ P[FRT]82B $scrib^{1}$ (n=10)

(Fig 2V) *y,w,eyFLP1/w*, *UAS-p35*; *Act5C>y⁺>Gal4*, *UAS-GFP*/*UAS-E2F*, *UAS-Dp*; P[FRT]82B *Tub-Gal80*/ P[FRT]82B $scrib^{1}$ (n=14)

(Fig 2W) *y,w,eyFLP1/w* or Y; *Act5C>y⁺>Gal4*, *UAS-GFP*/*UAS-dMyc*; P[FRT]82B *Tub-Gal80*/ P[FRT]82B $scrib^{1}$ (n=12)

(Fig 2X) *y,w,eyFLP1/w* or Y; *Act5C>y⁺>Gal4*, *UAS-GFP*/*UAS-dAkt*; P[FRT]82B *Tub-Gal80*/ P[FRT]82B $scrib^{1}$ (n=9)

(Fig 2Y) *y,w,eyFLP1/w* or Y; *Act5C>y⁺>Gal4*, *UAS-GFP*/+; P[FRT]82B *Tub-Gal80*/ P[FRT]82B $scrib^{1}$, $lats^{X1}$ (n=18)

(Fig 2Z) y,w,*eyFLP1/w* or Y; *Act5C>y⁺>Gal4*, *UAS-GFP*/*UAS-dAkt*; P[FRT]82B Tub-Gal80/ P[FRT]82B $scrib^{1}$, $lats^{X1}$ (n=16)

(Fig 4C) *y,w,eyFLP1/w* or Y; *Act5C>y⁺>Gal4*, *UAS-lacZ*/ *G454*, *UAS-Ras*^{V12}; P[FRT]82B *Tub-Gal80*/ P[FRT]82B

(Fig 4E) *y,w,eyFLP1/w* or Y; *Act5C>y⁺>Gal4*, *UAS-lacZ*/ *G454*, *UAS-Ras*^{V12}; P[FRT]82B *Tub-Gal80*/ P[FRT]82B, $scrib^{1}$

Analysis of Tissues

Cephalic complexes of wandering third instar larvae were dissected and the pattern of GFP expression in mutant clones was carefully observed in eye/antennal discs, the brain, and the leg discs. The presence of GFP-expressing cells in other areas of the larvae was also noted with the exception of cells in the gonads and genital discs (as well as the leg discs for *eyFLP5* and wing discs for *eyFLP1.2*), as this was also observed in animals with wild-type and otherwise noninvasive clones. Invasive tumors were considered suppressed if the majority of animals could pupate, and the majority of dissected cephalic complexes had little (minor projections restricted to the anterior of the VNC, as in Figure 3B) to no GFP-expressing cells invading the VNC.

Transplantation

Transplantation of imaginal disc tissues into adult hosts was performed as previously described (*S1*), with the exception that flies were anesthetized with CO_2 rather than ether. Briefly, third instar eye imaginal discs were dissected in PBS, cut into small pieces, and injected into the abdomens of at least 2-day-old well-fed females. Individual females were placed in a vial with several males, and any females that died within the first day were discarded and not included in the mortality curve. Pictures of GFP-marked tissue were taken every other day, and GFP expression away from the primary tumor was recorded. For the mortality curve, 15 animals of each genotype were analyzed. For internal organ analysis, 3 animals of each genotype were dissected on day 6 or 12 after transplant.

Immunohistochemistry

Double and triple immunofluorescent labeling of third instar imaginal discs was performed according to standard protocol and was visualized using FITC-, CY5- or CY3-conjugated secondary antibodies (Jackson Labs). Tissues were mounted in a manner whereby cross-sections of epithelial layers could be visualized, and all analyses were performed on undifferentiated cells in the eye-antennal disc anterior to the morphogenetic furrow. α-DCAD1 (rat monoclonal antibody against *Drosophila* E-cadherin) was from T. Uemura (1:20). Rhodamine-conjugated phalloidin was from Sigma (1:100). α-βGalactosidase (1:400) was from ICN Biomed. α-Laminin rabbit antiserum (1:100) was

generated with a combination of the synthesized Laminin A peptides RKIYATATCGPDTDGPELYCKGGGC, CGGGMINITPNMVVGDIWQGYCPLN, and CGGGKYIVAPDVILFSEHNALVHTS.

Supporting Text

Transplantation has been previously used to demonstrate that *lethal giant larvae* (*lgl*) and *discs large* (*dlg*) brains and wing discs can form secondary tumors (*S1*), implying that in *Drosophila* a single mutation may be sufficient to cause metastatic behavior. However, as tissues are cut into small pieces before transplantation, tumor formation could be aided by the disruption of basement membrane structure; interestingly, these mutant tissues have not been shown to exhibit invasiveness into adjacent tissues or to cause secondary tumor formation *in situ*. Also, as we have shown for *scrib*, clones of these mutant cells do not grown well in the presence of wild-type tissues (Fig. 2C), and not all discs in zygotically mutant animals are capable of overgrowth (Fig. 2D, *S2*, *S3*). The overgrowth phenotypes present in zygotically mutant *scrib*, *lgl*, and *dlg* larvae may be in part due to the disruption of signaling through nonautonomous factors such as Dpp, whose expression is perturbed in *lgl* mutants. This may explain why overgrowth in homozygous mutant animals is not recapitulated in mosaic clones.

Transplantation experiments were used to confirm whether the observed *in situ* behaviors of mutant cells could occur in a different environment. Transplanted tissues can be cultured in adult flies for several weeks, allowing ample time for tumors to invade host tissues. Transplantation of GFP-labeled $Ras^{V12}/scrib^{-/-}$ tumor fragments into the abdomens of wild-type adult females resulted in rapid tumor growth, caused a pronounced swelling of the abdomen, and quickly killed the host (Fig. S1E and S1Q). Interestingly, this swelling was also seen in larvae with mosaic clones (*S3*), suggesting that $Ras^{V12}/scrib^{-/-}$ cells could elicit an ascites-like host response. Control flies transplanted with tissue fragments only expressing Ras^{V12} did not die as quickly, and never exhibited the swelling response to the transplant (Fig. S1A and S1Q). Animals transplanted with disc fragments containing either wild-type or *scrib* loss of function cells did not die from the transplant, and the GFP-labeled tissue grew very slowly (Fig. S1I and S1Q, *S3*).

Previous experiments have shown that some transplanted tumors can give rise to the appearance of secondary growths in distant locations such as the head. In our hands, we found that the appearance of such secondary growths was variable, which may be dependent upon the amount of primary tissue injected and the degree to which it or host tissues are disrupted during the process of transplantation. In contrast to these secondary focal points of growth, we detected a clear genotype-correlated invasive behavior when internal tissues from host animals were examined. Transplanted tissues with cells expressing Ras^{V12}, like those with wild-type or *scrib* loss-of-function cells, were present as distinct free-floating masses in the hemolymph (Fig. S1B and S1J). However, $Ras^{V12}/scrib^{-/-}$ tumors observed at the same time after transplantation were consistently

attached to host tissues (Fig. S1F). Examination of host ovaries and intestines revealed GFP-positive cells both in developing ovarian follicles and the intestinal wall, suggesting that $Ras^{V12}/scrib^{-/-}$ cells migrated into and invaded these tissues (Fig. S1G and S1H). Such behavior was not observed for Ras^{V12} or *scrib* single mutant cells (Fig. S1C-S1D, S1K-S1L). These data are consistent with the metastatic behavior observed in the genetically mosaic larvae carrying $Ras^{V12}/scrib^{-/-}$ cells, indicating that the invasive phenotype was due to an intrinsic ability of these cells.

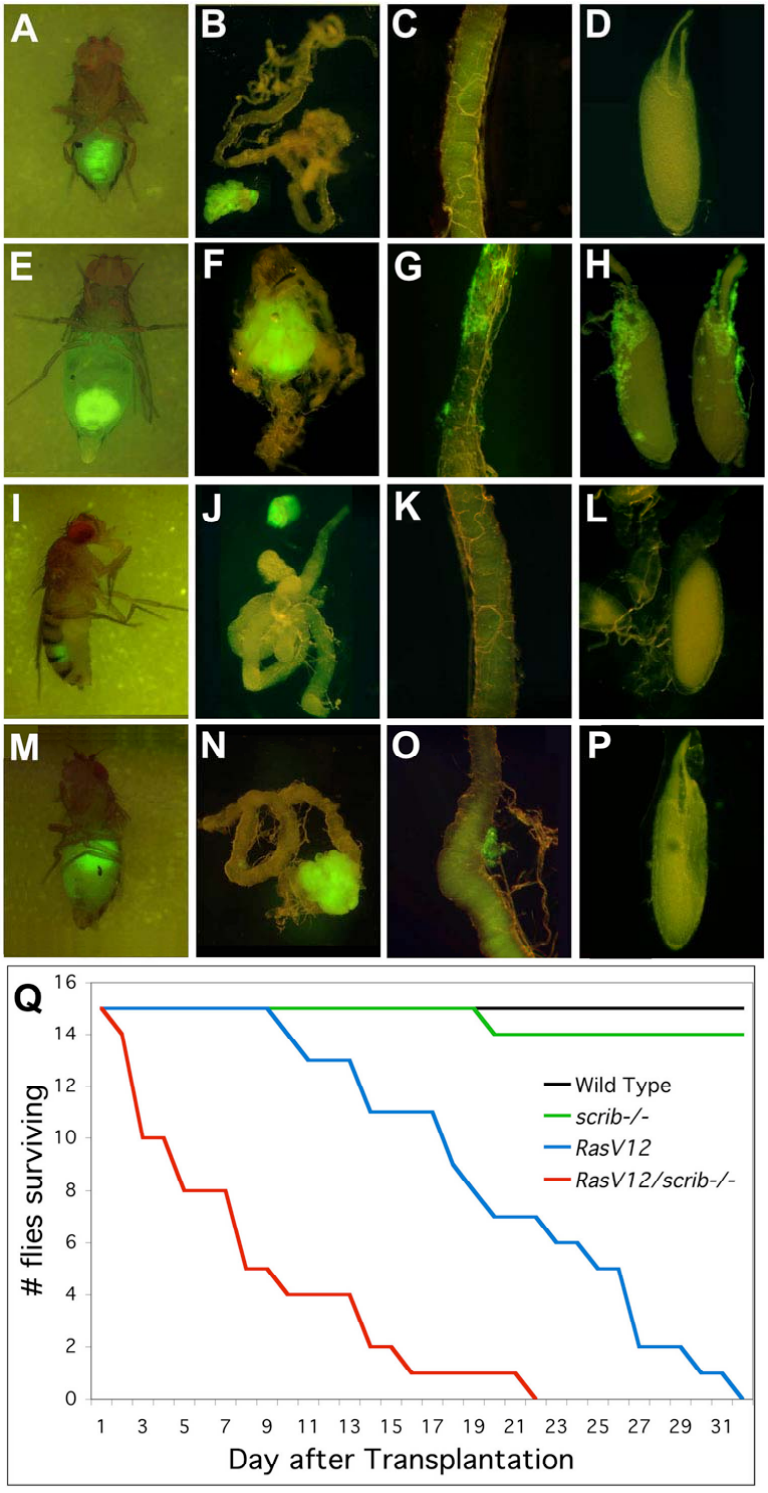

Fig. S1. Transplanted Tumor Phenotypes

Transplantation of Ras^{V12} (A-D), $Ras^{V12}/scrib^{-/-}$ (E-H), $scrib^{-/-}$ (I-L), and $Ras^{V12}/shg^{-/-}$ (M-P) eye disc tissues (green) into wild-type hosts. Adult females 6 days (A, E, M) or 12 days

(I) after transplantation, their dissected intestines with the transplanted tissue (B, F, J, N), close-up of intestine near the transplant (C, G, K, O), and dissected ovarian follicles (D, H, L, P). Only *Ras*^{V12}/*scrib*$^{-/-}$ tumor cells could spread onto the intestines and invade ovarian tissues of the host, although *Ras*^{V12}/*shg*$^{-/-}$ cells occasionally attached at discrete points (G-H, O). There is a dramatic host response to *Ras*^{V12}/*scrib*$^{-/-}$ tumor tissues, which results in a clear, swollen abdomen (E). Mortality of transplanted flies (Q).

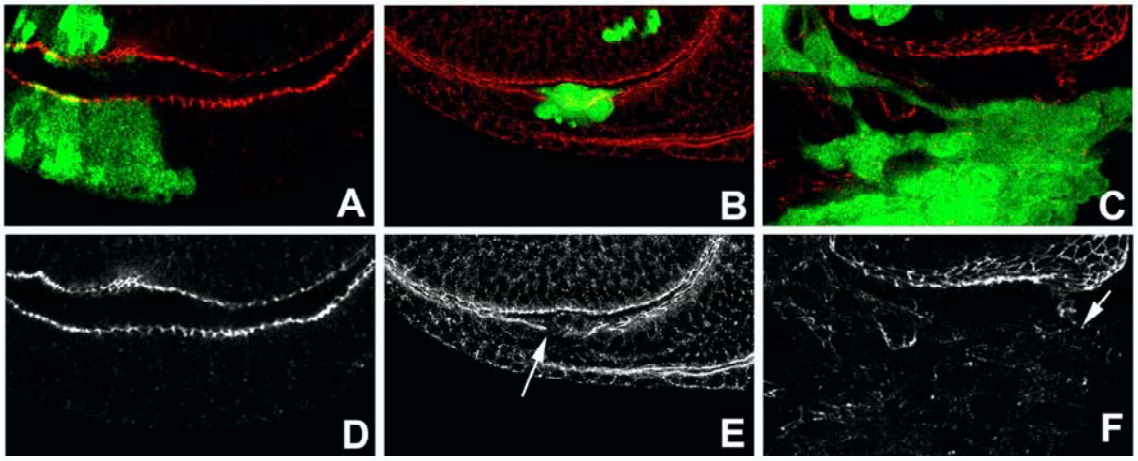

Figure S2. Loss of E-cadherin expression in *Ras*^{V12}/*scrib*$^{-/-}$ tumors

Mutant clones (green) of *Ras*^{V12} cells (A), *scrib* cells (B), and *Ras*^{V12}/*scrib*$^{-/-}$ cells (C) in eye-antennal discs stained for E-cadherin (red). E-cadherin staining alone is also shown below each image (D-F). All pictures were taken anterior to the morphogenetic furrow, where cells remain undifferentiated, and discs were mounted to allow cross-sectional view of epithelial cells. Arrow in E indicates the border of the *scrib* mutant clone. Loss of *scrib* causes an alteration of normal E-cadherin expression, and this alteration is greatly exacerbated in *Ras*^{V12}/*scrib*$^{-/-}$ cells.

References

S1. E. Woodhouse, E. Hersperger, A. Shearn, *Dev Genes Evol* **207**, 542-50. (1998).

S2. N. Arquier, L. Perrin, P. Manfruelli, and M. Semeriva, *Development* **128**, 2209-20. (2001)

S3. R. Pagliarini and T. Xu, unpublished data.